Dual phononic and photonic band gaps in a periodic array of pillars deposited on a membrane

Y. Pennec, Y. El Hassouani, C. Li, B. Djafari Rouhani, E.H. El Boudouti, H. Larabi, A. Akjouj
Institut d'Electronique, de Microélectronique et de Nanotechnologie, Université de Lille 1, 59655 Villeneuve d'Ascq, France

*Corresponding author: yan.pennec@univ-lille1.fr

Abstract: Phononic crystals are a class of materials that exhibit periodic variations in their density and elastic properties. Such crystals modify the propagation of acoustic waves and prohibit the propagation of sound for frequencies within the band gap. They have enabled exciting new ways to control sound in particular in the field of wave guiding and filtering, using point and linear defects introduced in the crystal, as well as in the field of sound isolation. In the photonic crystal counterpart, the medium is made up with a periodically modulation of the refractive index between their constituents. Their performance is determined by frequency gaps, forbidden for the propagation of the electromagnetic waves. In this work, we discuss the simultaneous existence of phononic and photonic band gaps in a periodic array of silicon pillars deposited on a homogeneous SiO_2 membrane.

Keywords: phononic, photonic, phoxonic, band gaps.

1. Introduction

Phononic crystals are a class of materials that exhibit periodic variations in their density and elastic properties [1, 2]. Such crystals modify the propagation of acoustic waves and prohibit the propagation of sound for frequencies within the band gap. They have enabled exciting new ways to control sound [3, 4]. Recently, an issue of interest is based on the study of phononic crystal slabs for potential applications as platforms for integrated technological circuits [6-10].

In the photonic counterpart, the medium is made up with a periodically modulation of the refractive index between their constituents also producing band gaps in which the propagation of electromagnetic waves is forbidden [11]. The existence of photonic band gaps for guided modes in periodic crystal slabs offers new possibility to control the light in integrated photonic devices [12-14].

The simultaneous existence of photonic and phononic band gaps and the confined phonon-photon interaction have been investigated in 1D multilayer structures [15]. In infinite 2D structures, relatively few works have been devoted to simultaneous control of phonons and photons [16, 17]. Some recent papers are also dealing with the opto-mechanical crystal slabs that sustain both the optical and mechanical excitations [18]. In two very recent papers, we and another group [19, 20] demonstrated the existence of dual phononic and photonic band gaps in 2.5D crystal plates composed of arrays of void cylindrical holes in silicon slabs with a finite thickness.

The main goal of this paper is to demonstrate the existence of dual phononic-photonic band gaps in the new type of structure constituted by a periodic array of pillars deposited on a layer of finite thickness. We concentrate our calculations on a structure where the pillars and the supporting plate are respectively made of silicon and silica (SiO_2). We investigate both the phononic and photonic band structures in three types of lattices, namely square, triangular and honeycomb and for a wide range of the geometrical parameters. In general, the phononic and photonic band structures are respectively calculated by finite element (FE) and by plane wave expansion (PWE) methods. However, finite difference time domain (FDTD) method has also been used to check the correctness and convergence of the results.

Section 2 describes the geometries considered in this paper as well as the methods of calculation. Section 3 contains the trends of the band gaps as a function of the lattice and the geometrical parameters for phononics and photonics respectively and presents the most appropriate geometries exhibiting dual band gaps. Conclusions are given in section 4.

2. Geometry and method of calculation

Figure 1(a) represents the general schematic view of the periodical structure of cylindrical silicon pillars deposited on a thin SiO_2 plate. The elastic constants and mass densities of the materials are given in Table I (see Appendix). The *z* axis is chosen to be perpendicular to the plate and parallel to the cylinder axis. By considering the lattice period *a* as the unit of length, there are several geometrical parameters involved in the problem, namely the height h_{Si} of the pillars, the thickness e_{SiO2} of the slab and the filling fraction *f*.

The phononic band structures are calculated by using the finite element (FE) method with the COMSOL Multiphysics finite element software. Only the solid materials are meshed (Fig. 1(b)) since elastic waves obviously cannot propagate in vacuum. Periodic boundary conditions, using the Bloch-Floquet equations, are applied at each side of the plate, assuming an infinite and periodic structure in the (*x*, *y*) plane.

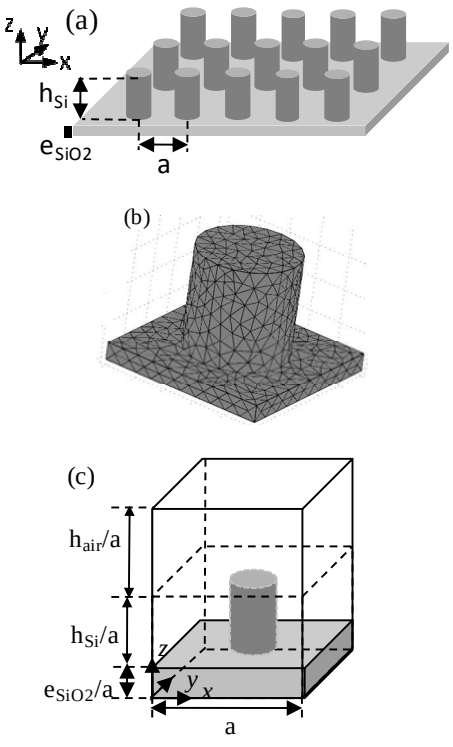

Figure 1. (a) Schematic view of the periodic crystal made up of cylindrical Si pillars on a SiO_2 plate. Representation of the unit cell used for: (b) the FE (phononic) and (c) the PWE (photonic) calculations.

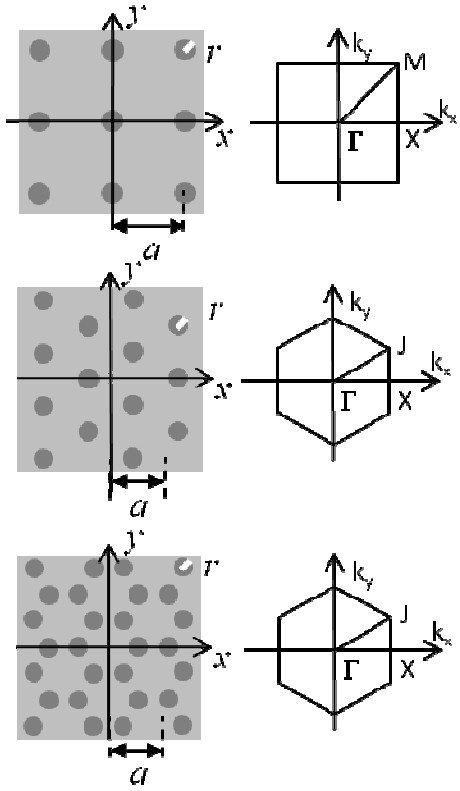

Figure 2. Square, triangular and honeycomb arrangements of the lattice crystal made up of silicon cylinders deposited onto a SiO_2 homogeneous plate and their corresponding Brillouin zone.

On the photonic side, the calculations of the dispersion curves are performed by using the developed PWE code with periodic conditions applied on each boundary of the unit-cell (see Fig. 1(c)). In this case, the thickness of the air slab separating neighboring photonic crystals in the *z* direction has been chosen such that to decouple them. Let us also mention that in the slab geometry, the photonic gaps have to be searched only below the light cone in vacuum. The air thickness has been chosen equal to h_{air}/a=4.0 to insure the stability of the whole branches under the light cone and the calculations have been performed with a number of plane waves equal to 2499. Calculations and convergences have also been checked using the finite difference time domain method (FDTD) with a good agreement.

As illustrated in figure 2, we have investigated several lattices, namely square, triangular and honeycomb where the corresponding Brillouin zones are represented in figure 2(b). The filling fractions of the cylindrical pillars are respectively given by $f = \frac{\pi r^2}{a^2}$, $f = \frac{2\pi r^2}{a^2\sqrt{3}}$ and $f = \frac{4\pi r^2}{a^2\sqrt{3}}$ for the square, triangular and honeycomb array, where r is the radius of the cylinder.

In both phononic and photonic cases, the wave vector is chosen along the high symmetry axis of the first Brillouin zone and the eigenfrequencies are obtained by solving the eigenvalue equation. In all the band structures presented in the paper, the frequencies are given in the dimensionless unit $\Omega=\omega a/2\pi c$ where c is the velocity of light in vacuum for electromagnetic waves and the transverse velocity of sound in silicon for elastic waves.

3. Phononic/Photonic band gaps

Figure 3(a) displays the map of the phononic band gaps for the three lattices as a function of the normalized height h_{Si}/a of the pillars, assuming a constant and relatively small value of the thickness of the plate e_{SiO2}/a=0.1. In all three cases, one can observe the opening of gaps (grey areas) as far as the height of the pillars exceeds 0.3a. In the frequency range of the Bragg diffraction, around [0.3, 0.5], we note the existence of two band gaps in all configurations. In the square and triangular lattices, these band gaps fall around nearly constant frequencies of Ω=0.35 and Ω=0.45, independently of the height of the pillars. These gaps are separated by a narrow pass band. The latter is essentially constituted by nearly flat branches associated to modes which are mainly localized at the corners of the unit cell inside the thin plate, without too much penetration into the pillars.

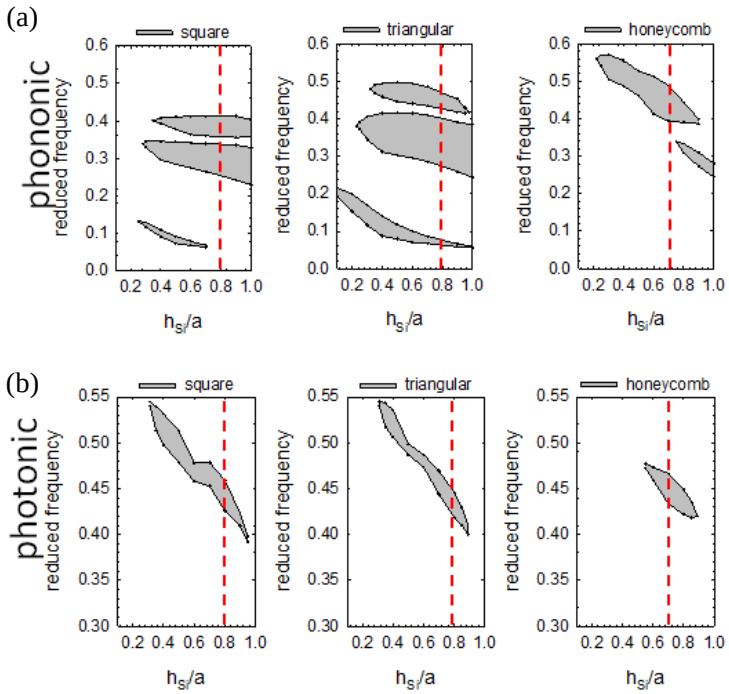

Figure 3 Evolution for the square, triangular, and honeycomb arrays of the phononic (a) and photonic (b) band gaps as a function of the height of the pillars h_{Si}/a, for e_{SiO2}/a=0.1 or h_{Si}/a=0.7. The filling factors of the pillars are kept at moderate values of f=0.4 (square), f=0.5 (triangular) and f=0.3 (honeycomb).

In addition, for the square and triangular lattices, a narrow gap can also exist at lower frequencies (Ω<0.2), much below the Bragg regime, where the wavelength in all constituting

materials is at least 10 times larger than the period of the lattice. The origin and existence condition of this gap, which presents some similarity with the behavior in locally resonant sonic material [4], was discussed in detail in ref. [8] for the square lattice geometry. In particular, it was shown that the existence of this gap requires a very thin plate ($e/a \approx 0.1$) and also the height of the pillars should be a moderate fraction of a as can be seen in Figure 3(a). The triangular lattice is the one that exhibits the largest gap over a wider range of the geometrical parameters. Let us remember [19, 20] that in a structure constituted by periodic holes in a Si membrane, the triangular lattice is not at all suitable to exhibit phononic band gaps.

We present Figure 3(b) the trends of the photonic band gaps maps as a function of the height h_{Si}/a of the pillars, for a constant value of the thickness of the plate $e_{SiO2}/a=0.1$. In all investigated lattices, one can see clearly the existence of a complete photonic gap (grey areas) which, however, closes faster than in the phononic case when increasing the height of the pillars. More precisely, for $e_{SiO2}/a=0.1$, the gap exists when the height of the pillars h_{Si}/a is chosen in the range [0.4, 0.9] for the square and triangular arrays and in the narrower range of [0.6, 0.8] for the honeycomb lattice. Actually, it would be desirable to have the frequency of the photonic gap as lowest as possible, which means choosing the highest possible values of h_{Si}/a around 0.7 to 0.8. Otherwise the gap covers only a very small area of the Brillouin zone just below the light cone and therefore becomes not very useful for practical applications.

We have clearly demonstrated the existence of complete phononic and photonic band gaps for the three investigated arrays of silicon pillars on a thin SiO_2 plate. The conditions on the geometrical parameters to obtain dual band gaps can be expressed as follows. For all arrays, the existence of a phononic gap requires heights of the dots higher than half time the lattice parameter. The existence of a photonic gap imposes to choose the height of the pillars as a fraction of the period ($h_{Si}/a \approx 0.4\text{-}0.9$). In practice, to avoid the photonic gap to occur only in a very restricted domain of the Brillouin zone just below the light cone, it would be suitable to decrease its frequency and therefore to choose the highest possible value of h_{Si}/a, around 0.8 (red dashed lines in Figs. 3).

Of course the actual frequencies in Figs. 3 scale inversely with the real dimensions of the structures. As an example, we can assume that the photonic midgap should occur at the telecommunication wavelength region around 1550 nm. Then all the geometrical parameters become totally determined and the corresponding phononic gap falls in the range of a few GHz.

4. Conclusions

We have theoretically demonstrated that a periodic array of silicon pillars deposited on a thin homogeneous SiO_2 layer exhibits dual phononic/photonic complete band gaps in the three most common lattices, namely square, triangular and honeycomb. The geometrical parameters appear to be quite compatible with the technological fabrication facilities. In addition, the triangular lattice is an interesting lattice in view of the creation of defects such as waveguides and cavities similarly to the case of usual photonic crystals. These properties will be investigated in subsequent works.

Phononic and photonic crystal slabs hold promises for the simultaneous confinement and tailoring of sound and light waves with potential applications to acousto-optical devices and highly controllable photon-phonon interactions. The new structure studied in this paper presents an alternative with respect to the more common structure constituted by a periodic array of air holes in a silicon membrane. In the latter case, it has been shown [22,23] that a complete photonic gap occurs only for a restricted range of the geometrical parameters in the honeycomb and boron nitride lattices, while for a wide range of parameters the phononic gap is accompanied only by a photonic gap with a given polarization (odd or even). Instead, in the case of pillars, the complete gaps can exist over a wide range of parameters. In addition, it is not required to choose a relatively high filling fraction, in contrast to the case of air holes in silicon.

5. References

1. M.S. Kushwaha, P. Halevi, L. Dobrzynski and B. Djafari-Rouhani, Phys. Rev. Lett. **71**, 2022 (1993).
2. M.M. Sigalas and E.N. Economou, Solid State Commun. **86**, 141 (1993)..
3. Y. Pennec, B. Djafari-Rouhani, J. O. Vasseur, H. Larabi, A. Khelif, A. Choujaa, S. Benchabane, and V. Laude, Appl. Phys. Lett. **87,** 261912 (2005).
4. Z. Liu, X. Zhang, Y. Mao, Y.Y. Zhu, Z. Yang, C.T. Chan, and P. Sheng, Science **289**, 1734 (2000).
5. J.C. Hsu and T.T. Wu, Phys. Rev. B **74**, 144303 (2006).
6. C. Charles, B. Bonello, and F. Gannot, Ultrasonics **44**, 1209(E) (2006).
7. J.O. Vasseur, P.A. Deymier, B. Djafari-Rouhani, Y. Pennec, and A.C. Hladky-Hennion, Phys. Rev. B **77**, 085415 (2008).
8. Y. Pennec, B. Djafari-Rouhani, H. Larabi, J.O. Vasseur, and A.C. Hladky-Hennion, Phys. Rev. B **78**, 104105 (2008).
9. T.T. Wu, Z.G. Huang, T.-C. Tsai, and T.C. Wu, Appl. Phys. Lett. **93**, 111902 (2008).
10. Y. Pennec, B. Djafari-Rouhani, H. Larabi, A. Akjouj, J. N. Gillet, J. O. Vasseur, and G. Thabet, Phys. Rev. B **80**, 144302 (2009).
11. E. Yablonovitch, J. Opt. Soc. Am. B **10**, 283 (1993).
12. S. G. Johnson, S. Fan, P. R. Villeneuve, J. D. Joannopoulos, and L. A. Kolodziejski, Phys. Rev. B **60**, 5751 (1999).
13. S. Shi, C. Chen, and D. W. Prather, J. Opt. Soc. Am. A **21**, 1769 (2004).
14. Y. Zhao and D. Grishkowsky, Optics letters **31**, 1534 (2006).
15. P. Lacharmoise, A. Fainstein, B. Jusserand, and V. Thierry-Mieg, Appl. Phys. Lett. **84**, 3274 (2004).
16. M. Maldovan and E.L. Thomas, Appl. Phys. Lett. **88**, 251907 (2006).
17. S. Sadat-Saleh, S. Benchabane, F.I. Baida, M.P. Bernal, and V. Laude, J. Appl. Phys. **106**, 074912 (2009).
18. A.H. Safavi-Naeini and O. Painter, Optics express **18**, 14926 (2010).
19. Y. Pennec, B. Djafari-Rouhani, E.H. El Boudouti, C. Li, Y. El Hassouani, J.O. Vasseur, N. Papanikolaou, S. Benchabane, V. Laude, and A. Martinez, Optics express **18**, 14301 (2010).
20. S. Mohammadi, A.A. Eftekhar, A. Khelif, and A. Adibi, Optics express **18**, 9164 (2010).

6. Acknowledgements

This work is supported in part by the European Commission Seventh Framework Programme (FP7) under the FET-Open project TAILPHOX N° 233833 and by Ministry of Higher Education and Research, Nord-Pas de Calais Regional Council and FEDER through the 'Contrat de Projets Etat Region (CPER) 2007-2013'.

7. Appendix

Table 1: Physical characteristics of the used materials: ρ is the density, C_{11}, C_{12} and C_{44} are the three elastic moduli and n is the refractive index.

Constant	Silicon (Si)	Silica (SiO_2)
ρ (kg/m^3)	2331	2275
C_{11} (N/m²)	16.57×10^{10}	7.50×10^{10}
C_{12} (N/m²)	6.39×10^{10}	2.25×10^{10}
C_{44} (N/m²)	7.962×10^{10}	3.0×10^{10}
n	3.5	1.5